
SELF-ORGANIZING STRUCTURES AND NANOASSEMBLIES

Rational Optimization of an Aptamer Specific to the Surface of Lung-Cancer Cells Using Mathematical Modeling and Small-Angle X-ray Scattering

P. V. Artyushenko^{a,c}, I. A. Shchugoreva^{a,c}, O. S. Kolovskaya^{a,c}, A. V. Rogova^{a,c}, R. V. Moryachkov^a, V. N. Zabluda^{a,b}, T. N. Zamay^{a,c,*}, A. V. Krat^{c,d}, R. A. Zukov^{c,d}, F. N. Tomilin^{a,b}, and A. S. Kichkailo^{a,c}

^aKrasnoyarsk Science Center, Siberian Branch, Russian Academy of Sciences,
Krasnoyarsk, 660036 Russia

^bKirensky Institute of Physics, Siberian Branch, Russian Academy of Sciences,
Krasnoyarsk, 660036 Russia

^cVoino-Yasenetsky Krasnoyarsk State Medical University,
Krasnoyarsk, 660022 Russia

^dKryzhanovsky Krasnoyarsk Regional Clinical Oncology Dispensary,
Krasnoyarsk, 660133 Russia

*e-mail: annazamay@yandex.ru

Received December 7, 2023; revised April 2, 2024; accepted April 9, 2024

Abstract—Aptamers, short oligonucleotides, are capable of high-affinity binding to targets due to their unique structure. Shortening the aptamer while maintaining the active site will increase the affinity and reduce the cost of synthesis. Using the example of the aptamer LC-224, a method for rational optimization of its length and verification of the validity of the developed approach is tested. The use of computer modeling and small-angle X-ray scattering shows the possibility of optimizing the aptamer structure by removing nucleotides that do not participate in binding to the target. It is shown that truncation of the aptamer does not reduce the affinity and specificity of the DNA aptamer. Thus, theoretical and experimental studies demonstrate successful experience in optimizing the structure of a DNA aptamer by shortening it without compromising its affinity and specificity for its target.

DOI: 10.1134/S2635167624600731

INTRODUCTION

Aptamers are single-stranded DNA or RNA that are able to bind with high affinity and specificity to various targets due to the formation of a unique three-dimensional structure [1]. They usually consist of 15–100 nucleotides, although not all bases are involved in interaction with targets [2, 3], it is extremely important to identify and shorten nonessential regions of the nucleotide sequence. Retaining only important nucleotides can significantly increase the affinity and selectivity of binding, as well as reduce the cost of aptamer synthesis [4]. Thus, the truncation of aptamers is a highly sought-after procedure. In most cases, truncation is done through empirical trial and error, resulting in a long chain of experiments. The replacement of some experimental stages of aptamer design with the joint use of small-angle X-ray scattering (SAXS) and molecular modeling can improve the efficiency of oligonucleotide-based drug development.

SAXS is used to determine the spatial structure of proteins and peptides, short DNA, RNA, and other biological objects in the range from 2 to 1000 nm in

the initial state [5, 6]. This method allows one to obtain information about the linear dimensions, molecular weight, volume and spatial shape of molecules, and, in combination with molecular modeling, determine the atomic structure of molecules. Thus, the combined use of computer modeling and SAXS is actively used to study the structure of compounds such as aptamers [7].

The purpose of this work is to determine the secondary and tertiary structures of the DNA aptamer LC-224 and truncation of its nucleotide sequence based on SAXS data and computer modeling.

EXPERIMENTAL

Molecular modeling. The LC-224 aptamer, which has affinity and specificity for biomarkers of lung adenocarcinoma to postoperative tissues, was obtained by us using the cell-SELEX technology and described in [8]. For both the full-length aptamer LC-224 and its shortened version LC-224t based on nucleotide-sequence data, we carried out the construction of sec-

ondary structures not only in the mFold program, but also in the OligoAnalyzer program [9]. Both programs produced identical models of possible secondary structures. The tertiary structures of aptamers were modeled using the SimRNA [10] and VMD [11] programs. Molecular dynamics calculations (MD) were performed in the GROMACS 2018.8 software package [12] with the Amber14sb force field [13] and water model TIP3P [14]. Aptamers are solvated in a cubic box. Na⁺ ions were introduced into the resulting cells to neutralize the negative charge of aptamers, as well as additional Na⁺ ions and Cl⁻ as a background electrolyte to a concentration of 0.15 M. 200-ns MD calculations were performed with the NPT ensemble (at a constant number of particles N , pressure P , and temperature T) at a temperature of 310 K and a pressure of 1 atm using a Berendsen thermostat and a Parrinello–Rahman barostat. For the obtained MD trajectories, cluster analysis was performed in the VMD program. MD calculations were carried out on the supercomputer of the Joint Supercomputer Center of the Russian Academy of Sciences (JSSC RAS).

Small-angle X-ray scattering. The SAXS data were obtained at the specialized station P12 BioSAXS of the European Molecular Modeling Laboratory (EMBL) on the Petra III storage ring of the DESY synchrotron, Hamburg, Germany.

A sample of DNA aptamer LC-224t in a PBS solution was prepared in a volume of 100 μ L with a concentration of 10 mg/mL, the solution was heated to a temperature of 90°C and cooled to 5°C to bring the conformation of the aptamer molecule into the most energetically favorable form. Next, the solution was placed in a size exclusion liquid chromatography system combined with a SAXS installation in the SEC-SAXS (Size-Exclusion Chromatography and Small-Angle X-ray Scattering) mode in order to exclude the influence of oligomers and aggregates formed in the solution. An Agilent 1260 Infinity instrument with a GE Superdex 75 Increase 10/300 chromatography column was used for chromatography. After passing through the column, the sample solution was placed directly under an X-ray beam of synchrotron radiation with a wavelength of 0.124 nm, which corresponds to a radiation energy of 10 keV. Each exposure was carried out with one-second exposures at a temperature of 20°C in the flow mode. 3600 frames were collected from the Dectris Pilatus 6M detector over a range of scattering angles $s = 0.2$ – 6.0 nm⁻¹ for 1 h of the experiment.

Programs from the ATSAS package were used to process and analyze the data. The chromatogram was analyzed in the CHROMIXS program and a SAXS graph was obtained, which was used for further processing. The size and volume of the molecule, and radius of gyration were calculated using the PRIMUS program [16] R_g , and a paired-distance distribution function is constructed $p(r)$. The DAMMIN program

constructs the shape of the total electron density of the molecule in the form of a ball model. The CRY SOL program compared the theoretically calculated SAXS signal from the molecular model of the aptamer with the experimental data.

Affinity and specificity analysis using flow cytometry. Work with human samples was carried out with the permission of the Local Ethics Committee of the Kryzhanovsky Krasnoyarsk Regional Clinical Oncology Center (Extract no. 6 from the minutes of meeting No. 55 of December 28, 2022). Postoperative materials were placed in a nutrient medium with an antibiotic and the study was carried out within 2 h from the moment of tissue collection. Postoperative lung-cancer tissue and relatively healthy adjacent tissue were crushed and passed through filters with a mesh size of 80 μ m. The study of the affinity and specificity of aptamers for postoperative lung-cancer tissues was carried out on a Beckman Coulter Cytomics FC 500 flow cytometer. FAM-labeled aptamers LC-224 and LC-224t were taken for analysis at a concentration of 100 nM; an aptamer nonspecific to lung-cancer tissue was used for control. The degree of fluorescence of aptamers bound to the target was assessed relative to the intrinsic basic fluorescence of intact cells without aptamers. The samples were prepared as follows: cells were incubated with 1 mg/mL mask RNA from baker's yeast (Yeast RNA, Sigma-Aldrich, USA) for 20 min, after which they were washed by centrifugation. Next, the cells were incubated with aptamers for 30 min on a shaker at room temperature, then washed to remove unbound oligonucleotides.

The proportion of targets bound to aptamers was determined by the fluorescence of aptamers in the green region of the spectrum on a flow cytometer. The fluorescence of intact cells was taken as the zero level. The true fluorescence of cell-bound aptamers was considered to be events above the zero-fluorescence level. Data analysis was carried out using a standard commercial flow-cytometry data-processing program, Kaluza 2.1.

RESULTS AND DISCUSSION

The secondary structure of the LC-224 aptamer was obtained using the mFold web server. Three possible variants of folding the LC-224 sequence are presented in Fig. 1.

As can be seen, in all variants of the aptamer secondary structure there is a repeating motif formed by nucleotides from the 14th to the 46th. The rest of the nucleotide sequence, from the 47th to the 80th nucleotide, can form different structural motifs. The LC-224 aptamer sequence was shortened in such a way that the structure of the shortened aptamer coincided with the corresponding fragment of the full-length aptamer. The new truncated aptamer LC-224t included the region from the 11th to the 50th nucleo-

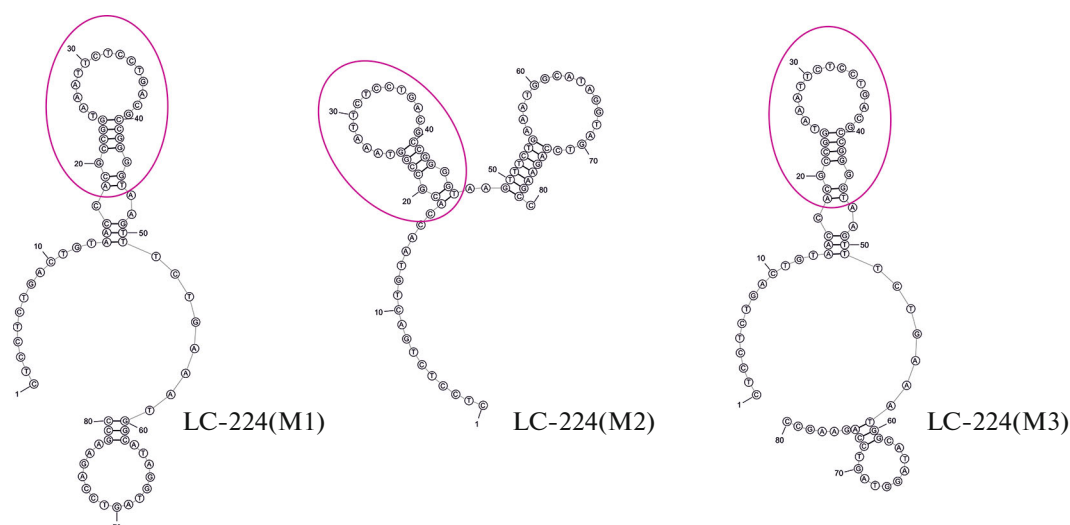


Fig. 1. Variants of the secondary structure of the LC-224 aptamer obtained using the mFold program.

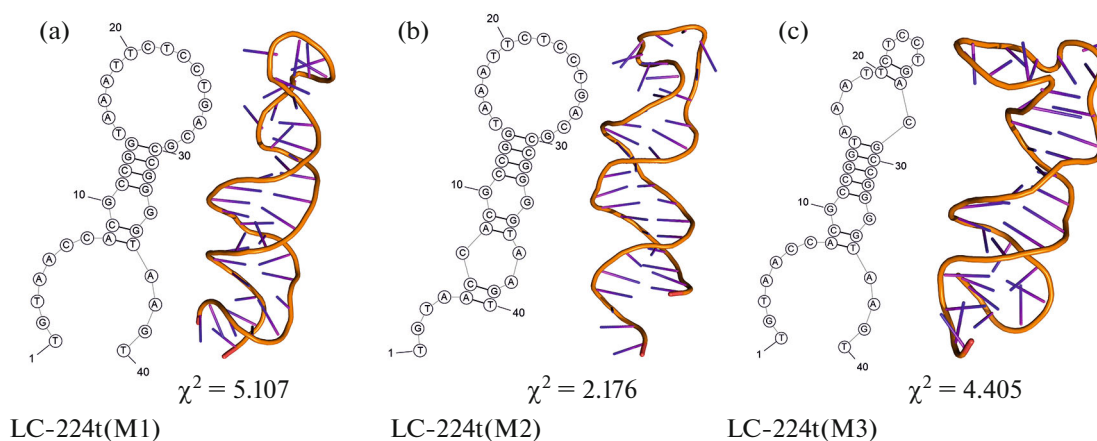


Fig. 2. Variants of the secondary and tertiary structure of the LC-224t aptamer.

tide of the original aptamer LC-224. For the LC-224t aptamer, three possible secondary structures were simulated using the mFold program, generally repeating the structure of the corresponding part of the LC-224 aptamer (Fig. 2).

The LC-224t aptamer was synthesized, and its structure was studied in solution by SAXS. Using the SEC-SAXS mode, a monodisperse solution was obtained, with which SAXS measurements were carried out. As a result, the following structural characteristics of the molecule were obtained: radius of gyration $R_g = 2.3$ nm, maximum molecule size $D_{\max} = 8.5$ nm, and molecule volume $V_p = 18.4$ nm³, which corresponds to the molecular weight $M_w = 12.5$ – 14.2 kDa (based on different estimates). Since the expected molecular weight of the molecule is 12.3 kDa, we believe that the sample was in a monomeric state in

solution. Based on the data obtained, a ball structure was constructed (Fig. 3).

Using molecular-modeling methods, we determined which of the possible secondary-structure models corresponds to the structure of the LC-224t aptamer in solution. For three possible secondary structures of the LC-224t aptamer, the corresponding three-dimensional models were constructed, for which MD calculations were then performed with a duration of 200 ns. The tertiary structures of the LC-224t aptamer obtained as a result of the cluster analysis of MD trajectories are presented in Fig. 3. By comparing the LC-224t aptamer models with SAXS data, it was found that the LC-224t(M2) model has a better agreement with the shape of the aptamer in solution. The discrepancy between the experimental SAXS data and the theoretically calculated signal from this model turned out to be minimal, $\chi^2 = 2.176$. The secondary

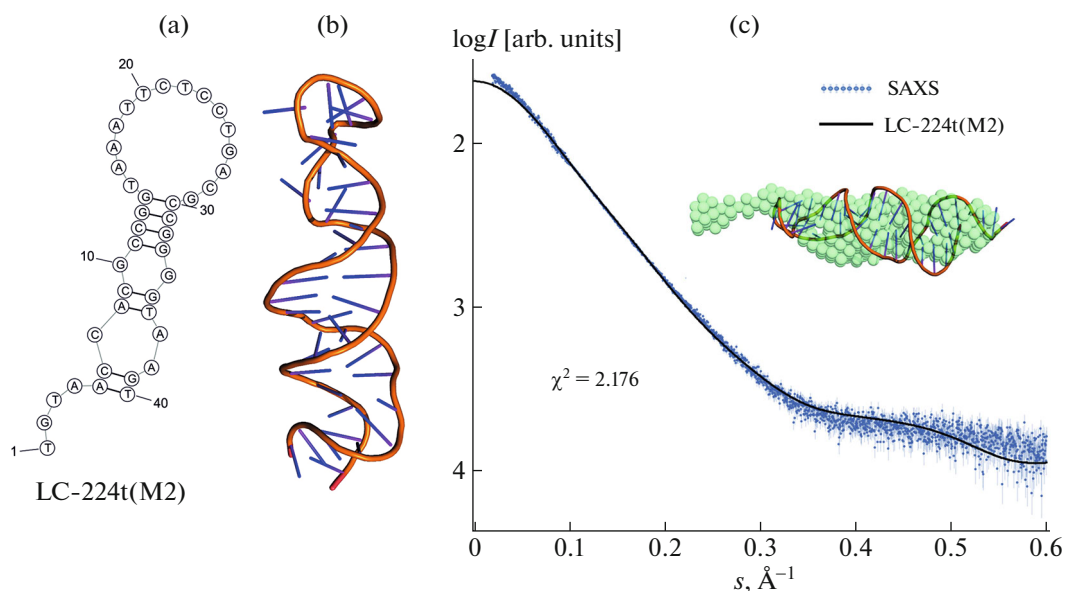


Fig. 3. Comparison of the LC-224t(M2) model with SAXS data: (a) secondary and tertiary model of the LC-224t (M2) aptamer, which best matches the experimental SAXS data; (b) experimental SAXS graph, depicted by points with a spread of errors, on which the theoretical SAXS curve from the three-dimensional aptamer model is superimposed, giving the smallest residual value $\chi^2 = 2.176$; (c) combination of the spherical structure of the total electron density of the aptamer molecule according to the SAXS experiment with a three-dimensional model of the molecule in a schematic display.

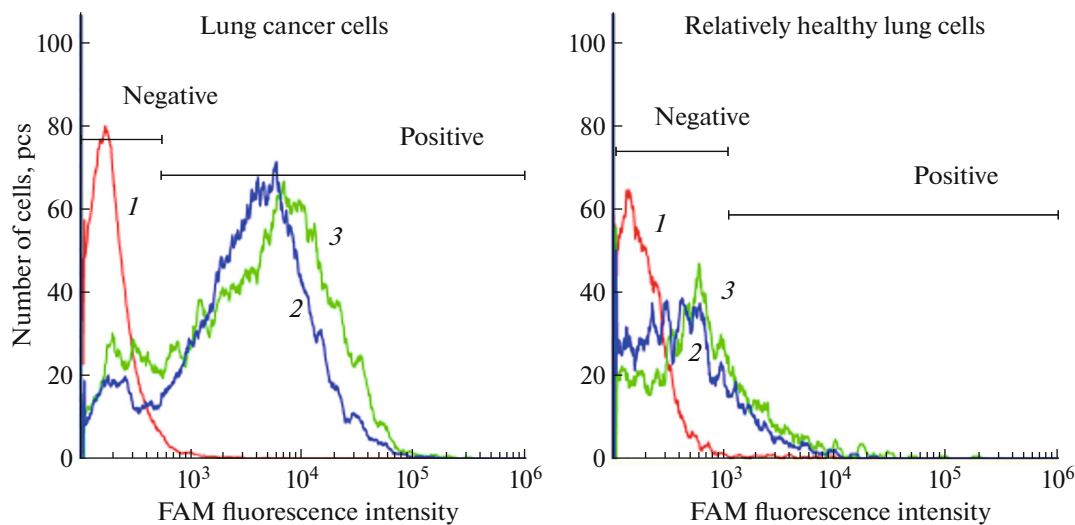


Fig. 4. Shortening the LC-224 aptamer did not affect its affinity and specificity: (a) binding of aptamers LC-224 and LC-224t to cells isolated from postoperative lung-cancer tissues, (b) binding of aptamers LC-224 and LC-224t to cells isolated from the postoperative tissues of relatively healthy lung tissues adjacent to cancerous ones; (1) unstained cells, (2) LC-224, (3) LC-224t.

structure, on the basis of which the LC-224t(M2) model was built, completely repeats the secondary structure of the corresponding fragment in the LC-224(M1) and LC-224(M3) models.

The affinity and specificity of the optimized aptamer was tested experimentally on postoperative lung-cancer tissues. It was shown that shortening did

not affect the ability of the aptamer to bind with affinity to lung-cancer cells (Fig. 4a); in experiments with healthy tissues, it also did not affect its specificity of interaction (Fig. 4a).

Recently, much attention has been paid to targeted therapy based on various nanoconstructs, which may include both molecules that perform a transport func-

tion and various functional groups. It is necessary to create such complexes with the minimum possible sizes so that they freely penetrate into the pathological focus and inside the cells. In addition, reducing the size of molecules increases their specificity and reduces the cost of synthesis. The combined use of computer modeling and SAXS makes it possible to optimize the structure of DNA aptamers by removing nucleotides that do not participate in binding. The SAXS method has proven itself well for studying the spatial structures of proteins, peptides, DNA, RNA, and their complexes in solution under quasi-physiological conditions. Its main advantages compared to other methods of structural analysis are ease of sample preparation, the ability to carry out measurements in liquid, small quantities and low concentration of the sample, and high speed of obtaining and processing experimental data. Computer modeling can speed up the optimization process and reduce its cost, since the researcher does not need to synthesize and test different versions of shortened aptamers. The proposed approach was tested on an aptamer for lung cancer.

CONCLUSIONS

The combined use of computer modeling and SAXS makes it possible to optimize the structure of DNA aptamers by removing nucleotides that do not participate in binding. Flow-cytometry analysis showed that the optimization procedure can be applied to DNA aptamers, since the parameters of their binding to lung-cancer cells and conditionally healthy cells did not change after optimization.

ACKNOWLEDGMENTS

We express our gratitude to the staff of the National Research Center “Kurchatov Institute” for scientific support of the project, the Center for Collective Use “Molecular and Cellular Technologies” of Voino-Yasenetsky Krasnoyarsk State Medical University and the Joint Supercomputer Center of the Russian Academy of Sciences (JSSC RAS).

FUNDING

The study was supported by the Russian Science Foundation (grant no. 21-73-20240).

CONFLICT OF INTEREST

The authors of this work declare that they have no conflicts of interest.

REFERENCES

1. X. Ni, M. Castanaris, and S. E. Lupold, *Curr. Med. Chem.* **18**, 4206 (2011).
<https://doi.org/10.2174/092986711797189600>
2. M. Jia, J. Sha, Z. Li, et al., *Food Chem.* **317**, 126459 (2020).
<https://doi.org/10.1016/j.foodchem.2020.126459>
3. X. Zheng, B. Hu, S. X. Gao, et al., *Toxicol.* **101**, 41 (2015).
<https://doi.org/10.1016/j.toxicol.2015.04.017>
4. A. Dhiman, A. Anand, A. Malhotra, et al., *Sci. Rep.* **8**, 17795 (2018).
<https://doi.org/10.1038/s41598-018-35985-1>
5. M. Hammel, *Eur. Biophys.* **41**, 789 (2012).
<https://doi.org/10.1007/s00249-012-0820-x>
6. R. P. Rambo and J. A. Tainer, *Annu. Rev. Biophys.* **42**, 415 (2013).
<https://doi.org/10.1146/annurev-biophys-083012-130301>
7. D. Morozov, V. Mironov, R. V. Moryachkov, et al., *Mol. Ther. Nucleic Acids* **25**, 316 (2021).
<https://doi.org/10.1016/j.omtn.2021.07.015>
8. G. S. Zamay, T. I. Ivanchenko, T. N. Zamay, et al., *Mol. Ther. Nucleic Acids* **6**, 150 (2017).
<https://doi.org/10.1016/j.omtn.2016.12.004>
9. M. Zuker, *Nucleic Acids Res.* **31**, 3406 (2003).
<https://doi.org/10.1093/nar/gkg595>
10. M. Magnus, M. Boniecki, W. Dawson, and J. M. Bujnicki, *Nucleic Acids Res.* **44**, W315 (2016).
<https://doi.org/10.1093/nar/gkw279>
11. W. Humphrey, A. Dalke, and K. Schulten, *J. Mol. Graph.* **14**, 33 (1996).
[https://doi.org/10.1016/0263-7855\(96\)00018-5](https://doi.org/10.1016/0263-7855(96)00018-5)
12. M. J. Abraham, T. Murtola, S. Roland, et al., *SoftwareX* **1**, 19 (2015).
<https://doi.org/10.1016/j.softx.2015.06.001>
13. J. A. Maier, C. Martinez, K. Kasavajhala, et al., *J. Chem. Theory Comput.* **11**, 3696 (2015).
<https://doi.org/10.1021/acs.jctc.5b00255>
14. W. L. Jorgensen, J. Chandrasekhar, J. D. Madura, et al., *J. Chem. Phys.* **79**, 926 (1983).
<https://doi.org/10.1063/1.445869>

Publisher’s Note. Pleiades Publishing remains neutral with regard to jurisdictional claims in published maps and institutional affiliations.